The Growth Rates and Densities of Ice Crystals between −3°C and −21°C

B. F. RYAN,[1] E. R. WISHART[1] AND D. E. SHAW[2]

CSIRO, Sydney, Australia

(Manuscript received 4 June 1975, in revised form 5 January 1976)

ABSTRACT

Ice crystals were grown in a supercooled cloud at temperatures ranging from −3°C to −21°C for periods from 30–40 s to 150–180 s. When the axial dimensions at a given time were examined as a function of temperature, there was a marked maximum along the *a* axis at −15°C and a secondary broader maximum along the *c* axis at −6°C. The growth of the axial dimensions can be adequately represented by a linear function of time.

A power function of time was fitted to the crystal mass growth measurements; these show a sharp maximum at −15°C and a secondary broader maximum at −7°C.

Crystal bulk densities estimated from the masses and axial dimensions vary with temperature in a complicated way, with a minimum of about 0.4 Mg m^{-3} at −5 and −17°C, and a maximum of 0.92 Mg m^{-3} (pure ice) at −3°C, and appear to be independent of time.

1. Introduction

A review of the literature reveals that present knowledge of the process by which ice crystals grow from vapor is uncertain and that there are, as yet, no reliable mathematical techniques to compute overall mass deposition rates. For example, although it is well established that ice crystal habits are markedly dependent on temperature and supersaturation (Hallett and Mason, 1958a; Kobayashi, 1961; Magono and Lee, 1966), there is some indication that the crystal habits are also altered by impurities or by the nucleant (Hallett and Mason, 1958b; Odencrantz, 1968). Also, measurements of the microscopic characteristics of growth have led to a reasonable description of the surface kinetics involved in the growth process (Lamb and Scott, 1972, 1974). There is little doubt that ice crystals grow by means of microscopic steps which possibly originate at emergent screw dislocations, and using appropriate parameters to describe the surface kinetics, the theory predicts the characteristic microscopic variations of crystal habits with temperature. However, mere prediction of the crystal habits is insufficient to allow calculations of the overall mass growth rates, because growth is dependent on the supersaturation field near the surface of the crystal.

Recent mathematical models (e.g., Jayaweera, 1971; Koenig, 1971) of ice crystal growth have been derived from current theory using parameters determined from field measurements. The alternative discussed here is to make laboratory measurements specifically for use in empirical models whose results can be directly compared with the predictions from complete physical models. However, for the most part this has been difficult, because when the crystals grow to an appreciable size they fall out of the relatively small laboratory cloud chambers (Fukuta, 1969).

Our present study attempts to extend ice crystal measurements to as large a time as possible with a large cloud chamber. This work is a continuation and an extension of the study (hereinafter referred to as I) reported by Ryan *et al.* (1974). The earlier paper reported measurements made in the temperature range between −5 and −9°C; the present measurements cover a broader temperature range (−3 to −21°C).

2. Experimental procedure

The techniques adopted in this new experiment were fundamentally the same as reported in I, except for the differences here noted: liquid water content (LWC) was maintained between 1 and 1.5 g m^{-3}, except at −15 and −17°C, where it was found necessary to increase the LWC to about 3 g m^{-3} to ensure that an adequate cloud was always present during the growth period, i.e., cloud droplet/ice crystal concentration ratio >5:1 (see I), so that water saturation could be assumed. A typical cloud droplet size distribution, as measured by a light-scattering instrument,[3]

[1] Division of Cloud Physics.

[2] Division of Mathematics and Statistics.

[3] Axially scattering cloud droplet spectrometer, Particle Measuring Systems, Boulder, Colo.

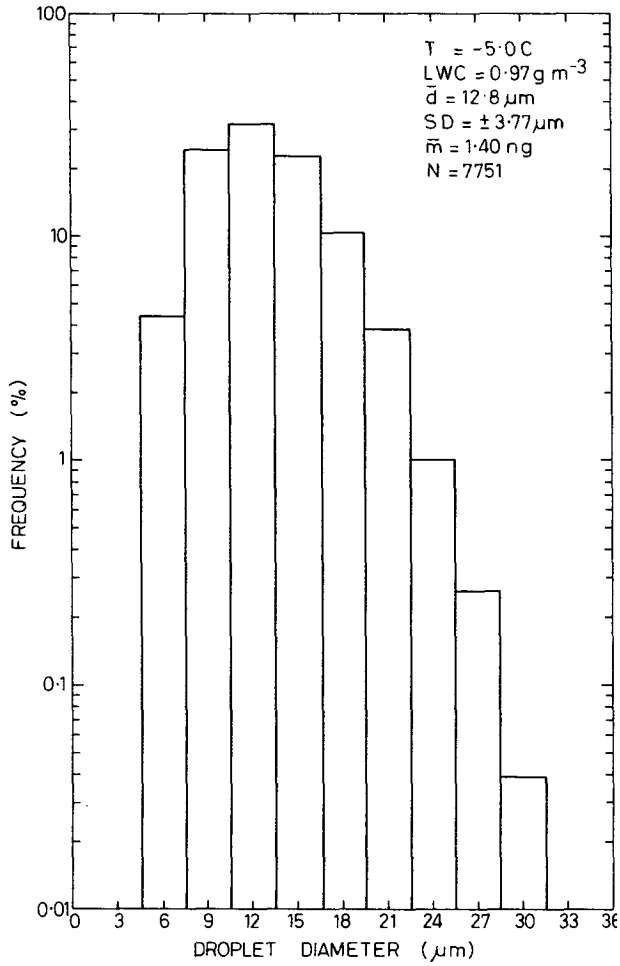

FIG. 1. Size distribution of cloud chamber droplets. T is temperature, LWC cloud liquid water content, $\bar{d}$ mean diameter of cloud chamber droplets, SD standard deviation of mean diameter, $\bar{m}$ mean mass, and N total droplet count.

is shown in Fig. 1. There were essentially no changes in the distribution for changes in LWC or temperature.

In the plate regime only a small fraction of the crystals landed "edge on" on the sampling slide and this made the technique of simultaneously measuring the crystal diameter, thickness and mass difficult. It was found more convenient to carry out separate experiments to measure each parameter as a function of temperature and time.

Ice crystals were produced below −3°C by bursting small plastic "bubbles" (used in packaging) in a syringe (see I). At −3°C the "popping bubble" technique no longer produced crystals. Therefore, at this temperature seeding was carried out by inserting into the cloud chamber a pin chilled in liquid nitrogen. By varying the time the pin was left in the chamber the numbers of crystals produced could be adjusted to numbers comparable with those produced by the "popping bubble," which were in the range 5–20 cm^{-3}.

Crystal aggregates were encountered at −15 and −17°C, the majority of which were no more than a pair of radiating assemblages of plates (Magono and Lee, 1966, plate 7a). This aggregation probably oc-

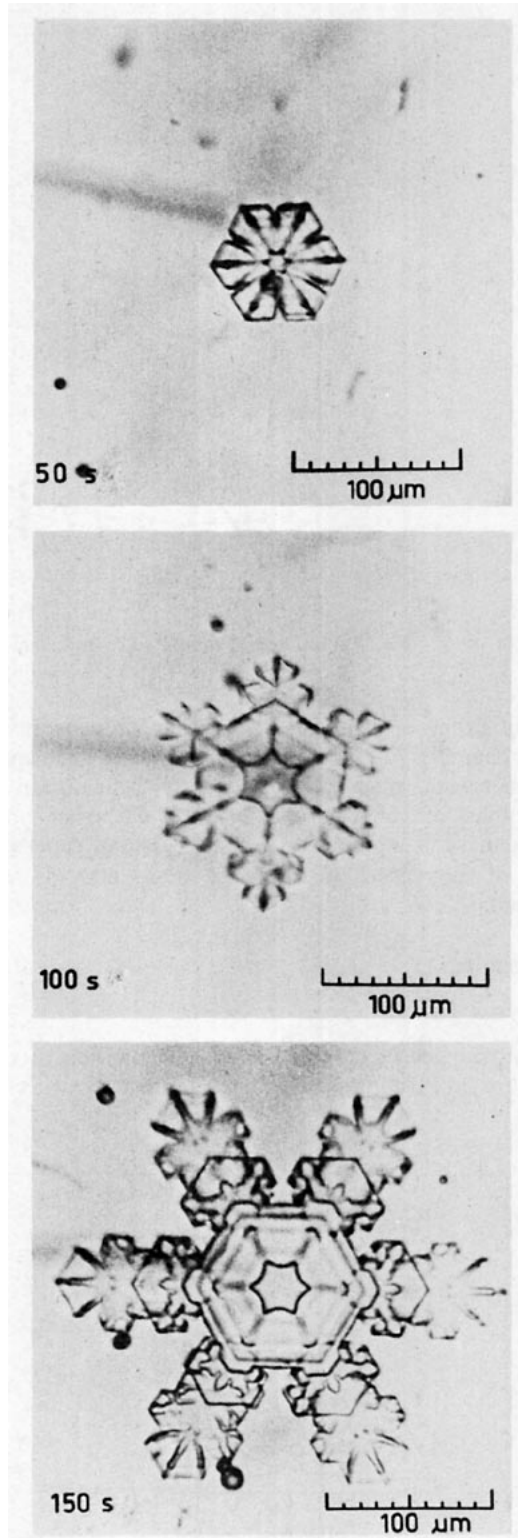

FIG. 2. Microphotographs of crystals at a temperature of −17°C, for sampling times of 50, 100 and 150 s after seeding.

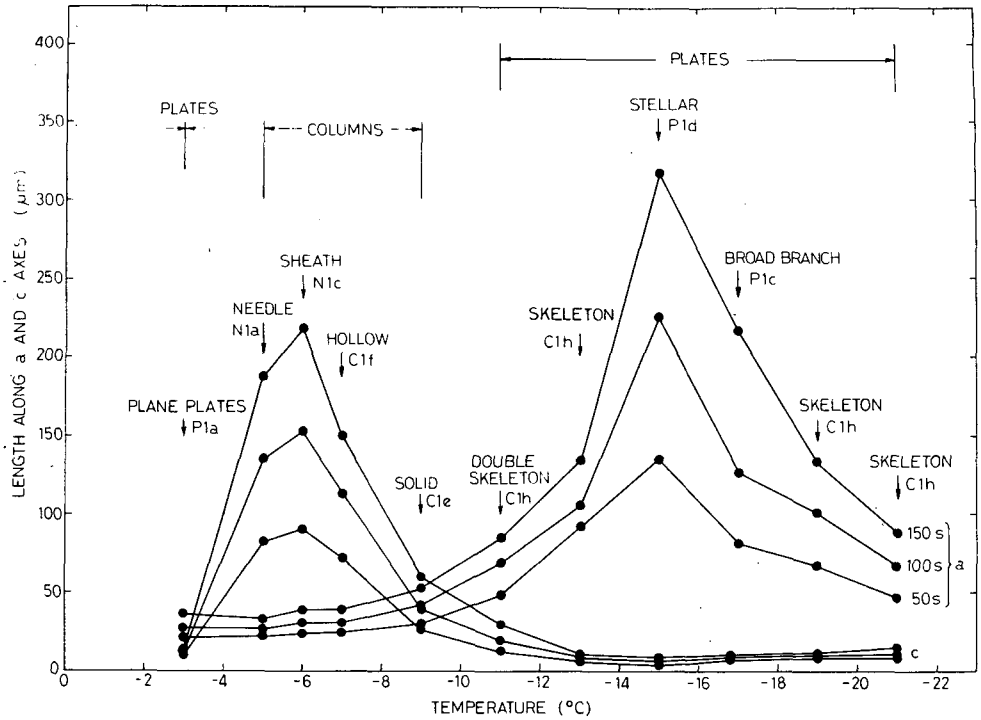

FIG. 3. Variation of estimated crystal axial dimensions with temperature at 50, 100 and 150 s after seeding.

curred either on the oiled sampling slide or in the cloud chamber just prior to sampling. The subsequent melted crystal mass was divided by 2 to obtain the mean mass of an individual crystal, which was similar to the mass of a single crystal. Very small concentrations of aggregates of three or more crystals were rejected.

3. Results

a. Crystal habits

The changes in crystal habit as a function of temperature are fundamentally in agreement with the laboratory studies of Hallett and Mason (1958a) and Kobayashi (1961) and the field observations of Ono (1970) and Auer and Veal (1970). A summary of crystal habits obtained is shown in Fig. 3, adopting the Magono and Lee classification. In our experiments more complicated structures, such as polycrystalline crystals, dendrites and capped columns were never observed. The observation of large numbers of polycrystalline crystals or assemblages of crystals at low temperatures by Fukuta (1969) may be associated with his technique of seeding with a chilled rod.

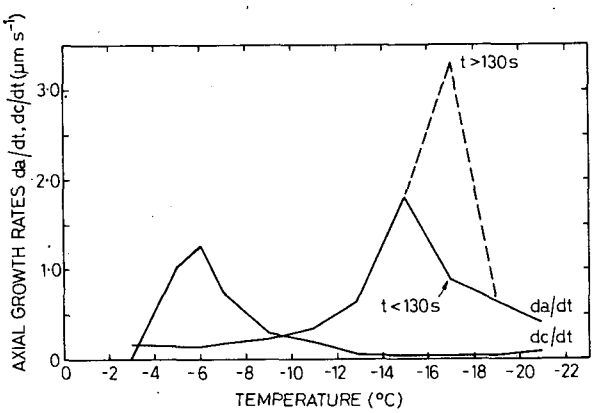

FIG. 4. Variation of estimated crystal axial growth rates with temperature.

b. Crystal dimensions and axial growth rates

As in I, it was found that, in general, single measurements of crystal dimensions were best fitted by a linear function of time, of the form

$$\left.\begin{aligned} a_d &= a_0 + \frac{da}{dt}t \\ c_d &= c_0 + \frac{dc}{dt}t \end{aligned}\right\}, \quad 30\text{ s} \lesssim t \lesssim 180\text{ s}, \tag{1}$$

where a_d and c_d are the lengths along the a and c axes, respectively, a_0 and c_0 are the intercepts, and t is time. The linear function provided an adequate fit; there was no statistical evidence to suggest the use of a more complex function (see the Appendix).

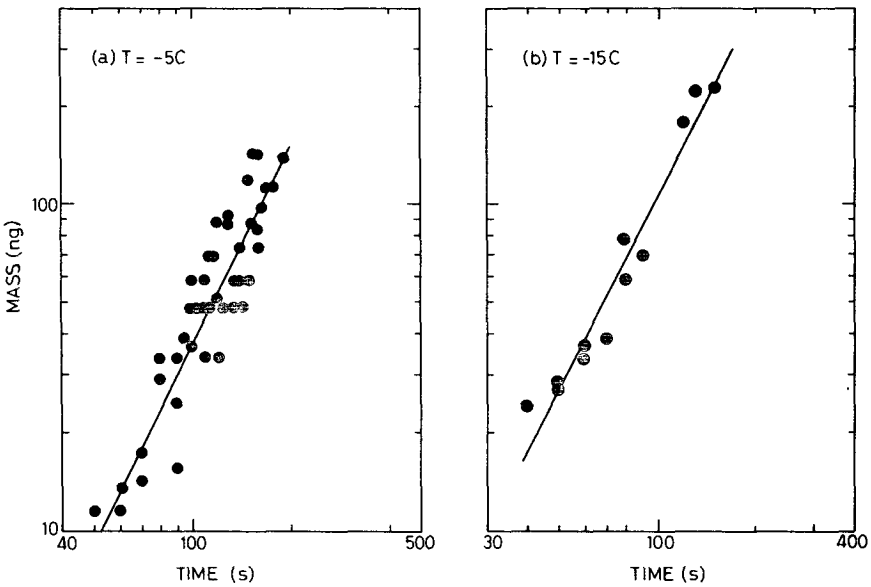

FIG. 5. Variation of crystal mass with time for temperatures of −5°C and −15°C. The lines represent the estimates of mass (see Tables 1 and 2).

However, at −17°C the *a* axis growth rates were found to increase markedly after about 130 s. Hence a simple linear fitting of the data was found to be inadequate and the data were better fitted with a pair of intersecting straight lines. This very marked increase in the growth rate along the *a* axis at −17°C about this time can be inferred from Fig. 2, and this increase corresponds with enhanced development of a broad-branched plate.

The fitted crystal dimensions for growth times of 50, 100 and 150 s and the estimated axial growth rates are shown in Figs. 3 and 4, respectively. Note the pronounced variation of the dimensions of the two axes with temperature, with a maximum in the growth along the *c* axis at −6°C and a very marked maximum in the growth along the *a* axis at −15°C.

c. Crystal masses and mass growth rates

The masses of individual crystals were measured (as in I) by melting the crystal and measuring the diameter of the resulting drop. It was found that a power law of the form

$$m_d = At^b, \tag{2}$$

where m_d is the crystal mass, A and b are constants, and t time, is statistically adequate in describing the data (see Fig. 5 and the Appendix). Approximately 95% confidence intervals for two temperatures are listed in Tables 1 and 2.

The crystal masses predicted by Eq. (2) at 50, 100 and 150 s are shown in Fig. 6. In addition, the mass growth rates were estimated by differentiating Eq. (2). Fig. 7 shows these estimated mass growth rates at 50,

TABLE 1. Variation of mean crystal mass with time, and the upper and lower 95% confidence limits, at a temperature of −5°C.

Time t (s)	Mean mass $\bar{m}$ (ng)	95% confidence limits	
		Lower limit	Upper limit
50	9.38	7.16	12.30
60	13.50	10.85	16.80
70	18.39	15.41	21.94
80	24.04	20.83	27.74
90	30.45	27.06	34.28
100	37.64	33.99	41.69
110	45.61	41.47	50.16
120	54.36	49.36	59.86
130	63.89	57.57	70.90
140	74.20	66.10	83.30
150	85.31	74.97	97.08

TABLE 2. Variation of mean crystal mass with time, and the upper and lower 95% confidence limits, at a temperature of −15°C.

Time t (s)	Mean mass $\bar{m}$ (ng)	95% confidence limits	
		Lower limit	Upper limit
50	27.45	22.63	33.29
60	39.11	33.55	45.60
70	52.80	46.27	60.25
80	68.51	60.33	77.79
90	86.23	75.37	98.66
100	105.98	91.25	123.07
110	127.73	107.98	151.09
120	151.50	125.59	182.77
130	177.29	144.07	218.17
140	205.10	163.46	257.34
150	234.92	183.73	300.37

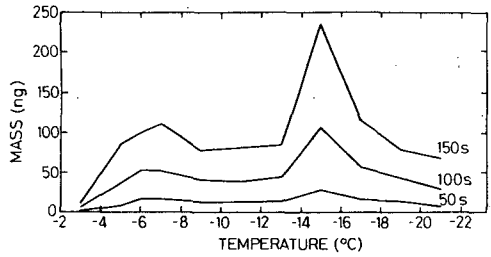

FIG. 6. Variation of the estimated crystal mass with temperature, at 50, 100 and 150 s after seeding.

100 and 150 s. It should be pointed out that the accuracy of these estimates is far less than that of the corresponding mass estimates because of the differentiating process; as yet, however, we have been unable to arrive at a reliable estimate of error in these mass growth rates.

A most important outcome in these results (the estimated masses in Fig. 6 and the estimated mass growth rates in Fig. 7) is the marked maximum at −15°C and a secondary broader maximum at −7°C.

d. Crystal densities

The experimental bulk densities of single crystals (ρ_e) were obtained with the following equation, where the crystal volume is modeled to a hexagonal cylinder:

$$\rho_e = \frac{m_e}{\frac{3\sqrt{3}}{8} a_e^2 c_e}. \tag{3}$$

Here a_e, c_e are the measured maximum dimensions along the a and c axes, respectively, and m_e is the measured mass. The expected crystal bulk densities (ρ_d) were calculated using values from Eq. (1) for the axial dimensions, and the masses calculated from Eqs. (2), i.e.,

$$\rho_d = \frac{Al^b}{\frac{3\sqrt{3}}{8} a_d^2 c_d}. \tag{4}$$

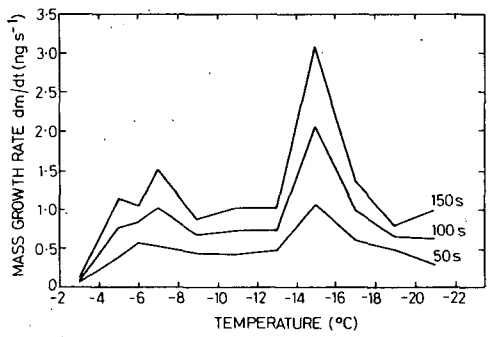

FIG. 7. Variation of the estimated crystal mass growth rates with temperature at 50, 100 and 150 s after seeding.

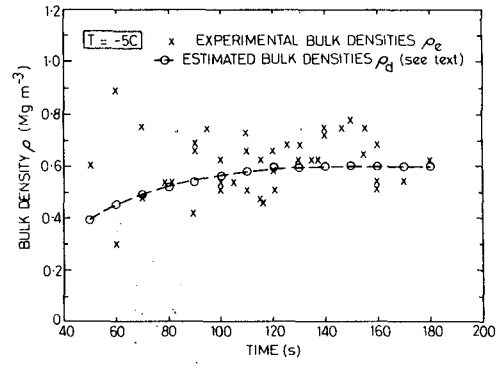

FIG. 8. Variation of crystal bulk density with time at a temperature of −5°C.

A comparison between results from (3) and (4) at −5°C shows (Fig. 8) that the two methods yield a similar result.

Fig. 9 shows a comparison between the bulk densities obtained from Eq. (4) and the experimental measurements of Fukuta (1969).

4. Discussion

a. Crystal axial dimensions

Auer and Veal (1970) and Ono (1970) measured the diameter of crystal replicas as a function of the crystal thickness for plates and of length for columns. Both sets of measurements cover much greater crystal size ranges and hence growth times. Auer and Veal fitted to most of their data (which covered a broader temperature range) a power law of the form $t = Ad^n$, where t is the thickness (or length), d the diameter of the crystals, and A and n are constants. The manner by which Ono obtained his fitted curve is not clear. As pointed out in I, at longer growth times ventilation may change the growth rates, and it is this that most probably leads to the nonlinear growth at the larger crystal sizes.

For the columnar regime between −5 and −9°C Fig. 10 shows a comparison between our fitted curves and those of Auer and Veal (1970) and Ono (1970). In this region, we find comparable axial dimensions; their curves closely approximate our linear fit. However, for the plate regime a direct comparison between our results and those of Auer and Veal and of Ono is more difficult, as they include in their data crystal habits other than simple hexagonal plates, stellars and broad-branched plates. In this regime, we observe thinner plates, which show only a small increase in thickness (the length along the c axis) with time (Fig. 11).

The change in habit at −17°C from simple hexagonal plates to broad-branched plates is very interesting, since this change corresponds to a change in the growth rate along the a axis. If the measurements were extended to longer growth times, other changes

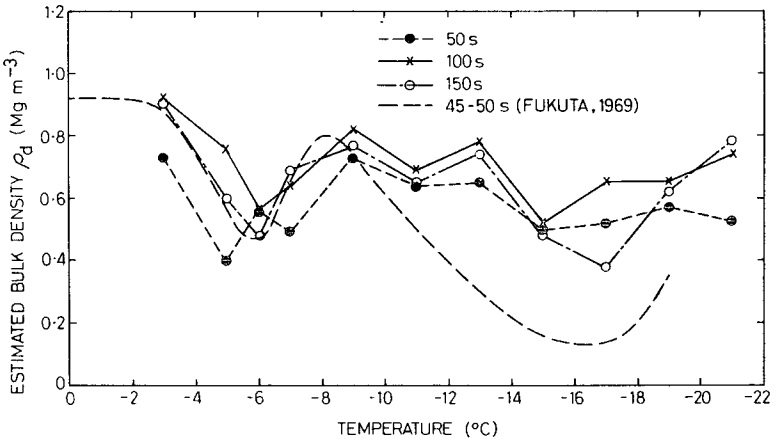

FIG. 9. Variation of estimated crystal bulk density with temperature at 50, 100 and 150 s after seeding. Dashed curve is based on Fukuta's (1969) measurements at 40–50 s after seeding.

in habit, such as a transition to dendritic crystals, may occur. However, such changes may be masked by the effects on the growth rate of increased ventilation.

b. Crystal masses and mass growth rates

The masses and mass growth rates both show a marked maximum at −15°C with a smaller secondary maximum at −7°C (Figs. 6 and 7). There have been only two other systematic measurements of crystal masses as functions of time and temperature against which the present results may be compared. Hallett (1965) examined large crystals (1–10 mm in diameter or length) growing in a diffusion chamber, while Fukuta (1969) measured crystals with growth times of less than 1 min, in a small cloud chamber. Most other earlier work is fragmented and has only reported results over a limited range of temperatures (Jayaweera, 1971). Both Hallett and Fukuta also observe a strong maximum in the growth rate near −15°C, and this is confirmed in our observations. However, the relative mass growth rates measured by Hallett varied by as much as two orders of magnitude with temperature. This relative effect is not shown in the present study; but the data trends definitely show pronounced increases in the relative maxima with time. Since Hallett's crystals were grown on a fiber under stagnant conditions for times as long as 1000 s and his crystals displayed dendritic growth characteristics (Hallett, private communication) that differed from what we observed, this result is not unreasonable.

Perhaps a more meaningful comparison can be made

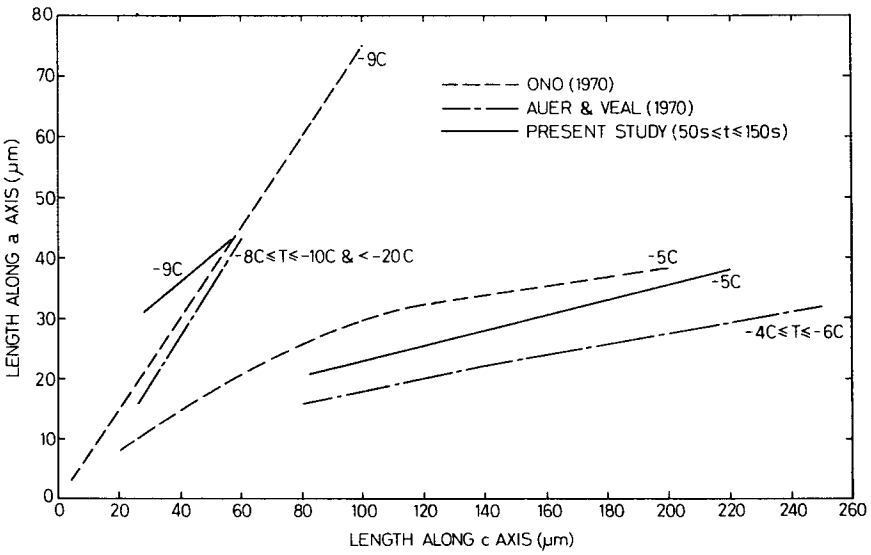

FIG. 10. Comparison of the estimated crystal axial dimensions with Auer and Veal's (1970) and Ono's (1970) field measurements at the temperatures indicated, for the columnar regime.

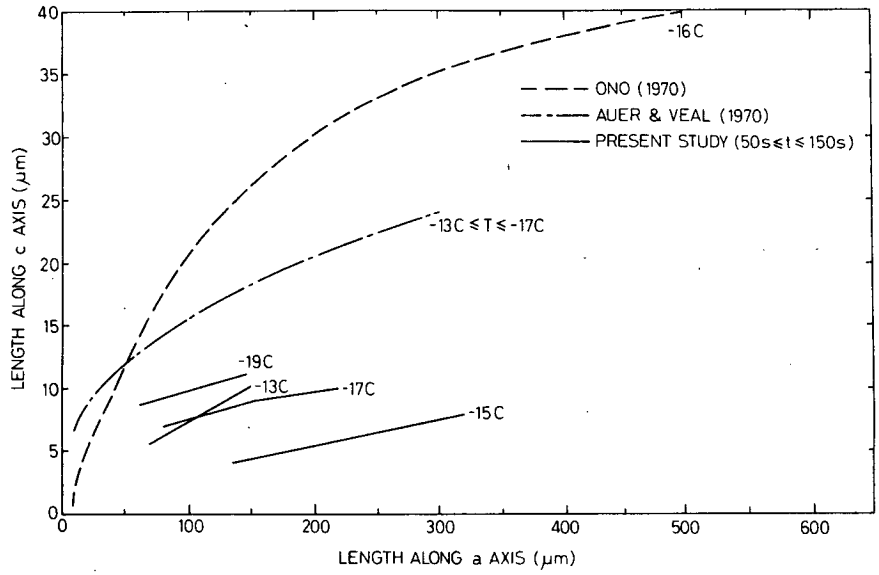

FIG. 11. As in Fig. 10 except for the plate regime.

with Fukuta (1969), where a comparison at a 50 s sampling time for masses is shown in Fig. 12. Fukuta obtained polycrystalline crystals at lower temperatures and this may well account for the higher masses obtained around the −15°C region.

c. Crystal densities

The deduced crystal densities all show evidence of a slow variation with time. However, these changes are of the same order as the approximate standard errors and so have little significance.

The variation of the crystal densities with temperature is similar to that reported by Fukuta (1969) in the temperature range −3 to −9°C. However, below −9°C our crystal densities are much larger than Fukuta's; this may simply result from his polycrystalline samples, but also it is not clear what volume he used to obtain bulk densities.

d. Comparison of mass and mass growth rates with existing numerical models

It is possible to compare the present experimental results with the previous diffusional models of crystal growth (e.g., Cotton, 1970; Jayaweera, 1971; Koenig, 1971). These models are formulated from earlier experimental measurements of crystal axial dimensions and bulk densities and from recent formulations of diffusional growth equations. They predict the pre-

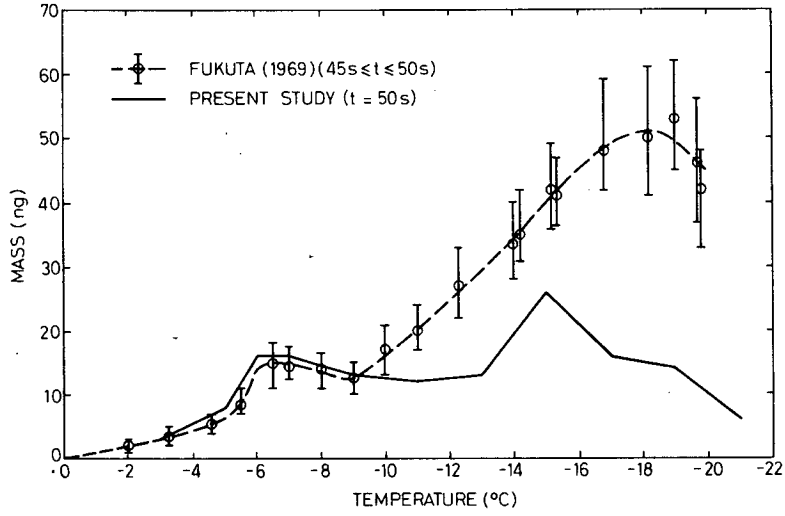

FIG. 12. Comparison of mass/temperature relationship of the estimated crystal mass at 50 s after seeding with Fukuta's (1969) experimental measurements at 45–50 s after seeding.

viously observed maxima in the mass growth rates. Fig. 13 shows the mean mass growth rates derived in this study at 150 s compared with the calculated mass growth rates of Jayaweera and Koenig. It should be noted that the results from Jayaweera and Koenig are based on the use of the field data described in their papers; a more valid comparison could be made if our own data had been employed.

The present measurements of crystal bulk densities, masses, and the derived mass growth rates emphasize the fact that caution is needed in numerical calculations of the mass of crystals as a function of time. If one wished to extrapolate to longer growth times, the present numerical procedures and data would provide results of doubful reliability.

It should be stressed that the axial dimensions, masses, growth rates and bulk densities obtained in this study are only valid for crystal growth time of less than 200 s. Further experimental measurements are now required to extend these times, where the effects of ventilation may play a dominant role, and should lead to the development of better numerical models.

5. Conclusions

These new experimental measurements of ice crystal growth at water saturation over the temperature range -3 to -21°C give information on axial dimensions, masses, axial and mass growth rates, and bulk densities for growth times up to about 200 s. Crystal habits obtained display the well-known transition of plate (-3°C) to column (-5 to -9°C) and plate (-11 to -21°C). Crystal axial dimensions increase as a linear function of time, except at -17°C, where a sudden increase in the a axis growth rate occurs at about 130 s, corresponding to a change in habit from a simple plate to a more complex broad-branched plate. Crystal axial dimensions show a sharp maximum along the a axis at -15°C of 316 μm and a secondary, broader maximum along the c axis at -6°C of 218 μm for a growth time of 150 s. Axial growth rates show a maximum along the a axis at -15°C for growth times $t<130$ s, shifting to -17°C for $t>130$ s. A smaller maximum is observed along the c axis at -6°C. A power function of time was fitted to the measured crystal masses. A marked maximum was shown at -15°C of 234 ng and a secondary broader maximum at -7°C of 110 ng, for a growth time of 150 s. The estimated crystal mass growth rates also display similar peaks at these temperatures. Comparison between the measured and estimated crystal bulk densities gave similar results; both display a very varied function of temperature, with a minimum of about 0.4 Mg m^{-3} at -5 and -17°C corresponding to close to the maximum of the axial dimensions and masses. The bulk densities appeared to be independent of time.

Comparisons of axial dimensions with field observations show reasonable agreement in the columnar regime (-5 to -9°C); but in the plate regime (-13 to -19°C) thinner plates were observed in this study.

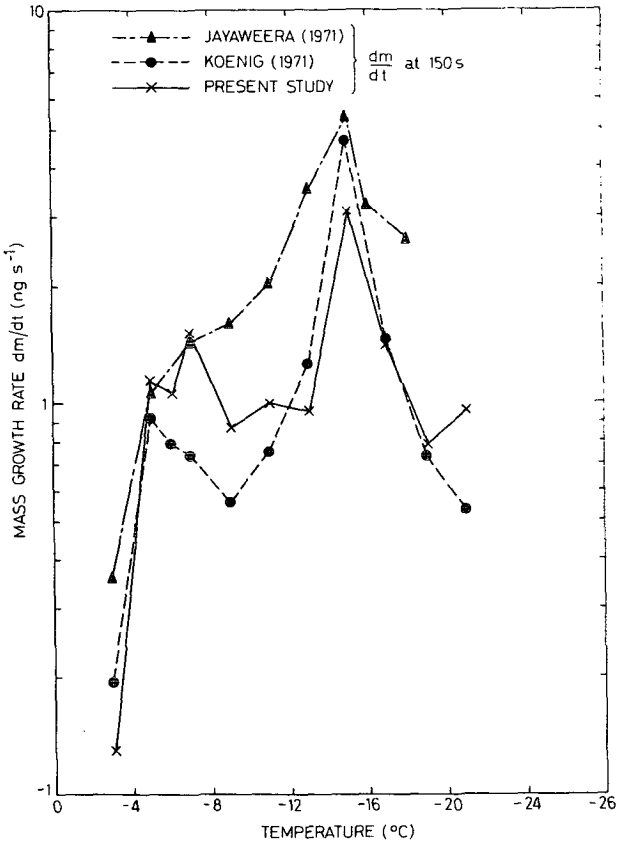

FIG. 13. Comparison of the estimated crystal mass growth rates with the numerical model calculations of Jawayeera (1971) and Koenig (1971) for a 150 s growth time at the temperatures shown.

Acknowledgments. The authors are extremely grateful to Drs. W. D. Scott and J. Hallett for their criticisms and valuable suggestions made in the preparation of this paper.

APPENDIX

Statistical Analysis of Data

Straight lines were employed to represent the growth of the axial dimensions of crystals as a function of time for each temperature investigated. Since multiple observations of the dimensions were available at many of the observational times, it was possible to perform a lack-of-fit test at a given temperature, using an F-test. [Broadly, this compares an estimate of variance obtained from the residuals about the fitted line with an estimate obtained from the repeated observations. Significant disparity between the estimates indicates that a straight line is not an adequate description of the data. See Draper and Smith (1966) for further details.] These tests were carried out at the 5% significance level, and in only one case in the

TABLE 3. Variation of estimated crystal bulk density and the approximate standard errors (see the Appendix) at a temperature of −5°C.

Time t (s)	Bulk density ρ_d (Mg m^{-3})	Standard error
50	0.5043	0.1367
60	0.5272	0.1103
70	0.5411	0.0883
80	0.5486	0.0703
90	0.5514	0.0561
100	0.5509	0.0460
110	0.5480	0.0401
120	0.5433	0.0382
130	0.5374	0.0396
140	0.5307	0.0428
150	0.5233	0.0469

temperature range −3 to −21°C was the fit significantly poor. This was at −17°C, where an adequate fit was provided by two intersecting straight lines, the intersection being estimated at a time of 130 s.

A power law was fitted to the individual measurements of the crystal masses by transforming to the logarithms of both mass and time, and fitting a regression line to these transformed variables. In general, there were not sufficient multiple observations to perform a reliable lack-of-fit test at every temperature. However, because more observations were available at −5°C, such a test could be carried out, and the linearity of the relationship between the logarithms of mass and time was satisfactory. Examination of the residuals at −5°C supported the fitting of a power law; such examinations as were possible at other temperatures also supported it.

The fitting of a linear relationship between the logarithms of mass and time is easily done. However, in this analysis we assume that the crystal mass has a log-normal distribution (Kendall and Stuart, 1963), which makes the estimation of the mean mass at a specified time difficult. We discuss briefly below the way in which we estimated mean mass.

In order to estimate the mean mass at a given time, and to provide an approximate 95% confidence interval for this mean, we have adopted the procedure of Patterson (1966). Suppose l represents log mass, $\hat{l}$ is the estimator of l obtained from the regression line, and σ_l^2 an estimate of the variance of the estimator $\hat{l}$. Then we estimate the mean mass $\bar{m}$ as

$$\bar{m} = \exp[\hat{l} + \tfrac{1}{2}\sigma_l^2], \tag{A1}$$

and the approximate 95% confidence interval (Δm) for the mean mass is given by

$$\Delta m = \exp(\hat{l} + \tfrac{1}{2}\sigma_l^2 \pm t_{95}\sigma_l), \tag{A2}$$

where t_{95} is the 95% point of a t-variate with the appropriate degrees of freedom. Tables 1 and 2 include the approximate 95% confidence intervals derived from Eq. (A2).

The estimators and intervals given above for the mean mass do not necessarily possess all the desirable properties of estimators and intervals derived directly from linear regression (Draper and Smith, 1966); for example, the distribution of the estimator $\bar{m}$ is skewed. The formula for the confidence interval is an approximation to a true 95% confidence interval. However, the formula was tested in a small simulation experiment and, for the situations in which it was used, it gave results reasonably consistent with the required level of 95%.

The densities were estimated by taking the estimated mass and dividing by the estimated bulk volume [obtained from the estimated axial dimensions using Eq. (1)], so that the distribution of the estimator of the density cannot be derived. However, Fig. 8 indicates that the bias is not substantial in the case at −5°C. In addition, we have used the formula given by Kendall and Stuart (1963) to calculate an approximate standard error for the estimator of density; these values are included in Table 3.

REFERENCES

Auer, A. H., and D. H. Veal, 1970: The dimensions of ice crystals in natural clouds. *J. Atmos. Sci.*, **27**, 919–926.

Cotton, W. R., 1970: A numerical simulation of precipitation development in supercooled cumuli. Ph.D. thesis, Pennsylvania State University; also Rept. No. 17, Dept. Meteor.

Draper, N. R., and H. Smith, 1966: *Applied Regression Analysis*. Wiley, 407 pp.

Fukuta, N., 1969: Experimental studies on the growth of small ice crystals. *J. Atmos. Sci.*, **26**, 522–531.

Hallett, J., 1965: Field and laboratory observations of ice crystal growth from the vapor. *J. Atmos. Sci.*, **22**, 64–69.

——, and B. J. Mason, 1958a: The influence of temperature and supersaturation on the habit of ice crystals grown from the vapor. *Proc. Roy. Soc. London*, **A247**, 440–453.

——, and ——, 1958b: Influence of organic vapors on the crystal habit of ice. *Nature*, **181**, 467.

Jayaweera, K. O. L. F., 1971: Calculations of ice crystal growth. *J. Atmos. Sci.*, **28**, 728–736.

Kendall, M G, and A. Stuart, 1963: *The Advanced Theory of Statistics*, Vol. I, *Distribution Theory*, 2nd ed. London, Griffin, 433 pp.

Kobayashi, T., 1961: The growth of snow crystals at low supersaturations. *Phil. Mag.*, **6**, 1363–1370.

Koenig, L. R., 1971: Numerical modeling of ice deposition. *J. Atmos. Sci.*, **28**, 226–237.

Lamb, D., and W. D. Scott, 1972: Linear growth rates of ice crystals grown from the vapor phase. *J. Cryst. Growth*, **12**, 21–31.

——, and ——, 1974: The mechanism of ice crystal growth and habit formation. *J. Atmos. Sci.*, **31**, 570–580.

Magono, C., and C. W. Lee, 1966: Meteorological classification of natural snow crystals. *J. Fac. Sci. Hokkaido Univ.*, Ser. 7, **2**, 321–335.

Odencrantz, F. K., 1968: Modification of habit and charge of ice crystals by vapor contamination. *J. Atmos. Sci.*, **25**, 337–338.

Ono, A., 1970: Growth mode of ice crystals in natural clouds. *J. Atmos. Sci.*, **27**, 649–658.

Patterson, R. L., 1966: Difficulties involved in the estimation of a population mean using transformed sample data. *Technometrics*, **8**, 535–537.

Ryan, B. F., E. R. Wishart and E. W. Holroyd III, 1974: The densities and growth rates of ice crystals between −5°C and −9°C. *J. Atmos. Sci.*, **31**, 2136–2141.